

Evaluation of Post-Fabrication Thermoforming Process for Intracortical Parylene Sheath Electrode*

Brian J. Kim, *Student Member, IEEE*, Seth A. Hara, *Student Member, IEEE*, Benny Chen, Jonathan T.W. Kuo, Curtis Lee, *Student Member, IEEE*, Christian A. Gutierrez, *Member, IEEE*, Tuan Hoang, Malancha Gupta, Victor Píkov, and Ellis Meng, *Senior Member, IEEE*

Abstract— The chemical, mechanical, and electrochemical attributes of the Parylene sheath electrode (PSE) were evaluated following a post-fabrication thermoforming process to determine its impact on both the polymer and thin film platinum materials. The three-dimensional conical shape of the PSE was formed via thermal molding of a surface micromachined Parylene C microchannel using a custom shape-forming microwire having the desired taper at 200°C for 48 hours under vacuum. Contact angle and Fourier transform infrared spectroscopy measurements indicated that the thermoforming process resulted in no significant changes to the surface and bulk chemistry of Parylene. The thermoformed Parylene samples possessed greater Young's modulus, but retained their flexibility. Electrochemical characterization of electrodes before and after thermoforming revealed a decreased storage charge capacity and increased electrode impedance, however, recording functionality was not lost as resolvable neuronal unit activity was successfully obtained post-implantation.

I. INTRODUCTION

Chronic implementation of intracortical prosthetic devices has been limited by multiple failure mechanisms encountered during long-term implantation. In addition to abiotic failure mechanisms (e.g. electrode corrosion, broken connectors), the decline of recording performance of electrodes has been attributed to biotic causes that occur *in vivo* [1]. Specifically, the inflammatory response caused by insertion trauma and the presence of a foreign body within the cortex [2, 3] forms glial cell encapsulation and neuronal retraction from the recording sites, which limit the longevity of high fidelity recordings [4]. This response is further exacerbated by the mechanical mismatch between current electrodes, made of silicon, metal, or stiffer polymers, and

the surrounding neural tissue, inflicting continuous damage during brain micromotion over time [5].

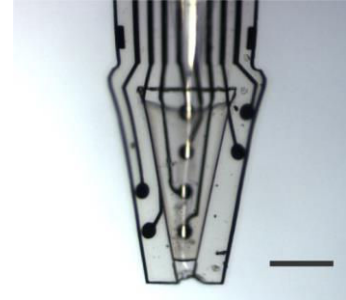


Figure 1. Optical micrograph of the tip of a Parylene sheath electrode. Scale bar is 300 μm .

To address these concerns, we developed a three-dimensional (3D), flexible Parylene sheath electrode (PSE) constructed from surface-micromachined Parylene C for neuronal recording (Fig. 1) [6]. The PSE consists of a hollow sheath structure with four electrode sites within the lumen and another four electrode sites on the outer perimeter of the sheath. The aim of the PSE is to utilize a drug-coated, sheath-based design to minimize the immune response and encourage neuronal proliferation and growth towards and within the sheath, which houses the electrode sites and follows the previous success of the neurotrophic cone electrode [7]. The PSE however, also has added benefits of a flexible, thin (10 μm) substrate material that would further reduce the mechanical mismatch (and subsequent damage) between the PSE and surrounding cortical tissue compared to the rigid, glass-based neurotrophic cone electrode.

To construct this 3D sheath structure from a flat, surface-micromachined device, we harness the thermoplastic property of Parylene C, and thermally mold, or “thermoform”, a conical shape from a flat microchannel [8]. Thermoforming these devices involves holding a sample in the desired configuration within a mold, and heat treating the assembly at a temperature between the glass transition temperature (~60-90°C) and the melting temperature (290°C) of Parylene C [9]. By annealing the assembly between these temperatures while maintaining the desired configuration, the polymer chains can rearrange and thereby facilitate conformation to the molded orientation. As the assembly is cooled and mold removed, the final molded configuration remains, due to the immobility of the polymer chains at temperatures below the glass transition temperature. It is important to note that the thermoforming process should be carried out in a vacuum environment to inhibit thermal oxidation of Parylene C at temperatures

*This work was sponsored by the Defense Advanced Research Projects Agency (DARPA) MTO under the auspices of Dr. Jack Judy through the Space and Naval Warfare Systems Center, Pacific Grant/Contract No. N66001-11-1-4207.

B.J. Kim, S.A. Hara, J.T.W. Kuo, C. Lee, T. Hoang, and E. Meng are with the Department of Biomedical Engineering at the University of Southern California, Los Angeles, CA 90089 USA (corresponding author: 213-821-3949; e-mail: ellis.meng@usc.edu).

B. Chen and M. Gupta are with the Mork Family Department of Chemical Engineering and Materials Science at the University of Southern California, Los Angeles, CA 90089 USA.

C. A. Gutierrez is an independent engineering consultant in Los Angeles, CA 90089 USA.

V. Píkov is with the Huntington Medical Research Institutes (HMRI), Pasadena, CA 91105 USA.

>125°C [10]. The PSE was thermoformed at 200°C for 48 hours to not only achieve its 3D shape, but also to enhance the adhesion between the Parylene C layers [11]. Here we present the evaluation of the thermoforming process on the chemical and mechanical properties of Parylene C as well as the electrochemical performance of the PSE, to capture any material changes and their possible impacts on the final thermoformed device, and on the feasibility of the PSE as an implantable intracortical neural probe. We seek to assess the advantages and disadvantages of this simple post-fabrication process for the development of novel 3D structures using Parylene C for applications in neural electrode development.

II. MATERIALS AND METHODS

A detailed description of the fabrication of the PSE was previously described [6]; a short description is presented here for completeness. Platinum electrodes and leads were e-beam evaporated and patterned by a liftoff method onto a Parylene C substrate layer on top of a silicon carrier wafer. A Parylene C microchannel was then constructed on top of the four inner electrodes by depositing a Parylene C layer on top of a sacrificial photoresist structure in the shape of a raised trapezoid. Openings were etched on the tip and base of this microchannel to allow for the insertion of the microwire mold for thermoforming. Lastly, the flat probes were oxygen plasma etched to their final shapes and were released from the wafers and soaked in acetone to remove the sacrificial photoresist structures to reveal the hollow microchannel to be thermoformed (Fig. 2a).

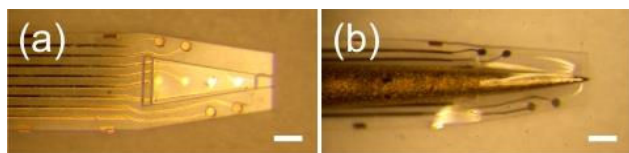


Figure 2. (a) Flat, surface micromachined Parylene device following removal of sacrificial photoresist. (b) Insertion of microwire mold into microchannel. Scale bars are 200 μm .

A. Thermoforming of Parylene Devices

Following removal of the sacrificial photoresist, a custom-made microwire mold of the desired taper width was manually inserted into the lumen of the microchannel to mechanically open and create the desired 3D conical structure (Fig. 2b). This assembly was then placed inside of a vacuum oven, where upon reaching maximum vacuum (~ 10 mTorr), the temperature was ramped 1.3°C/min to 200°C. Once the ramp was complete, the temperature was held for 48 hours, after which the oven was slowly cooled to room temperature overnight. Following the thermoforming process, the microwire was easily removed from the Parylene devices to reveal the 3D cone shapes (Fig. 3).

B. Chemical and Mechanical Characterization

Surface and bulk chemical changes to the thermoformed Parylene material were characterized using contact angle measurements and Fourier transform infrared spectroscopy (FTIR), respectively. These tests were conducted on unmolded Parylene test samples (15 μm thick films) that were also subjected to the same thermoforming process as microwire-molded samples. Mechanical changes were assessed by measuring the Young's modulus of heat-treated

Parylene samples using a nanoindenter with a Berkovich tip. A custom made large-scale indenter (>100 μm displacement) also conducted additional structural stiffness measurements to assess the mechanical resilience and flexibility of the newly thermoformed structure.

C. Electrochemical Characterization

Thermoforming effects on electrode (and thus recording) properties of the PSE were assessed using cyclic voltammetry (CV; 1x PBS, -0.6 to 0.8V, scan rate of 50 mV/s for 3 cycles, Ag/AgCl reference) and electrochemical impedance spectroscopy (EIS; 1x PBS, 1-100,000 Hz, Ag/AgCl reference), which are widely used to assess electrode properties and investigate changes to the electrode surfaces [12]. CV and EIS measurements were taken of electrodes before and after the thermoforming process to observe possible annealing effects on the electrode material, and give insight into the recording capability of the PSE.

D. In Vivo Chronic Implantation and Measurements

Chronic implantation of the PSE was performed in the M1 motor cortex of young male Sprague Dawley rats (>340 g). Electrophysiological recordings were carried out weekly, with rats anesthetized with Ketamine/Xylazine (90/10 mg/kg, IP). The electrophysiological data was acquired at 16 bit and 40 kHz per channel using a 64-channel data acquisition system (OmniPlex; Plexon Inc., Dallas, TX) and high-pass filtered at 300 Hz to remove the low-frequency fluctuations from the baseline.

III. RESULTS AND DISCUSSION

A. Thermoforming

Vacuum thermoforming of the Parylene C microchannels produced consistent 3D sheath structures without observable material oxidation. Different conical taper widths (sharp and moderate) were produced from Parylene microchannels and microwire molds of varying tapers, and a cylindrical structure was also formed by using a cylindrical microwire mold (Fig. 3a-c). A design iteration of the PSE with perforations on the sheath and substrate to facilitate inner-outer cell-to-cell signaling was also thermoformed using the same procedure to produce a 3D perforated sheath (Fig. 3d), demonstrating the robustness of the process in forming 3D sheath structures.

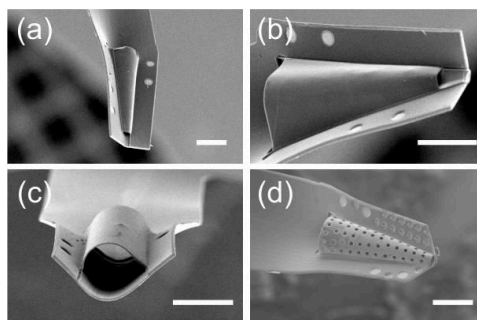


Figure 3. SEMs of thermoformed sheath structures showing different PSE designs: (a) sharp taper, (b) moderate taper, (c) cylindrical, and (d) perforated with sharp taper. Scale bars are 200 μm .

B. Chemical Characterization

Contact angle measurements of Parylene test samples indicated that the surface energies and surface roughness between untreated and thermoformed samples of Parylene were relatively unchanged following the thermoforming process (Table 1).

TABLE I. RESULTS OF CONTACT ANGLE MEASUREMENTS

Condition	Contact Angle
Untreated	$73.4 \pm 0.9^\circ$; Mean \pm SE, n = 3
Thermoformed (200°C, 48 hours)	$74.7 \pm 1.1^\circ$; Mean \pm SE, n = 3

The bulk material also remained consistent, as seen through absorbance measurements using FTIR (Fig. 4). There was no observable change in the bulk chemical functionality as no new significant peaks were detected between the untreated and thermoformed samples. These results suggest that the thermoformed films still retain the as-deposited Parylene C surface and bulk chemical properties, which is important to note when relying on the biocompatibility of as-deposited Parylene films.

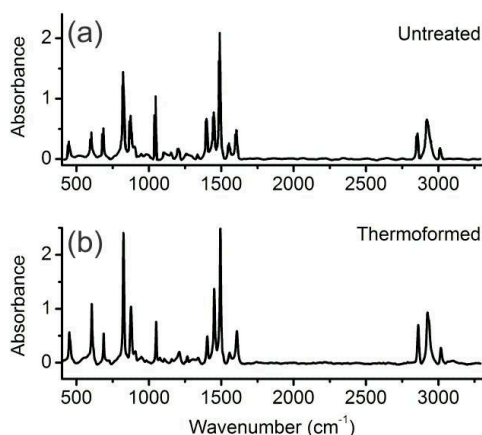


Figure 4. Comparison of FTIR results of (a) untreated and (b) thermoformed Parylene C samples indicating no new peaks following the thermoforming process.

C. Mechanical Characterization

Measurements of Young's modulus indicated that the Parylene substrate increased in stiffness following thermoforming (Table 2). These results are also consistent with the increase in crystallinity that is observed in literature with the heat treatment of Parylene due to the formation of additional crystalline domains within the amorphous regions of the polymer [13]. Previous studies have shown that this stiffness can be tuned by varying the parameters of thermoforming such as the temperature and duration of heat treatment [8].

TABLE II. RESULTS OF YOUNG'S MODULUS MEASUREMENTS

Condition	Young's Modulus
Untreated	2.70 ± 0.06 ; Mean \pm SE, n = 16 ^a
Thermoformed (200°C, 48 hours)	3.97 ± 0.06 ; Mean \pm SE, n = 28 ^a

a. n values taken at different test regions over a single large area sample

Though the Parylene substrate increases in stiffness following the thermoforming process, flexibility of the PSE was not lost. This is supported by mechanical deformation tests that demonstrated that the Parylene sheath structure could return to its original open position following a deformation of 200 μm imposed by a 25 mN load (Fig. 5). The sheath is also sufficiently robust to resist any deformation *in vivo* as seen in histological data [14]. Although slightly stiffer than the untreated material, the thermoformed PSE is still a large improvement in minimizing the mechanical mismatch between cortical tissue and current technologies, and compares favorably to other popular polymers used in microfabrication, such as polyimide.

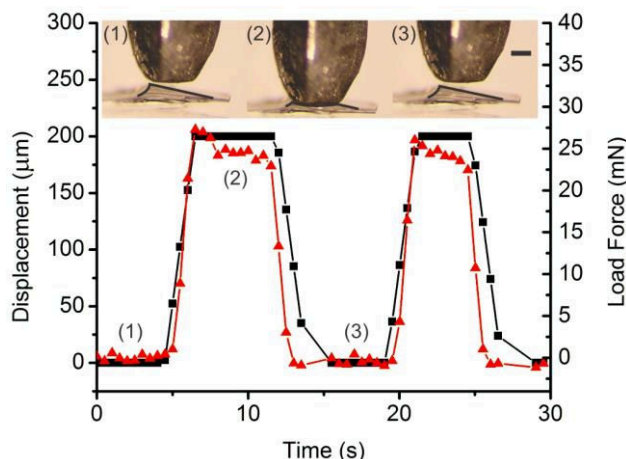


Figure 5. Displacement (black squares) and load force (red triangles) measurements taken during deflection studies of thermoformed PSE sheath structure. Inset and plot indicate the (1) starting position, (2) deflection of 200 μm , and (3) return to initial position indicating following release of load. Sheath remains flexible and is robust to mechanical perturbations. Sheath deformation is outlined in black to facilitate visualization. Scale bar is 200 μm .

D. Electrochemical Characterization

CV measurements of the platinum electrode surface indicated a noticeable reduction in the area inside the CV curve compared to the untreated electrodes, indicating a decreased charge storage capacity (Fig. 6).

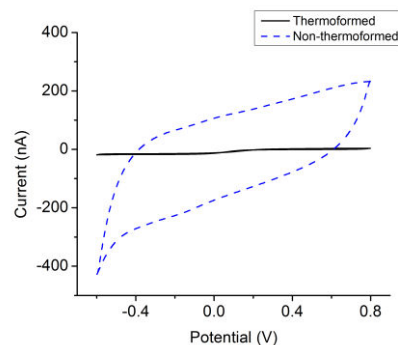


Figure 6. Representative CV curves of untreated (blue dashed) and thermoformed (black solid) electrodes.

Electrochemical impedance also supported an altered electrode surface as the impedance magnitude had increased and the phase plot had shifted to the right; the 1 kHz

impedance magnitude increased by 375% to ~125 k Ω following thermoforming (Fig. 7). Taken together with the CV results, we hypothesize that one or more phenomena may have contributed to the observed changes: (1) contamination of the surface of the platinum electrodes by chlorine molecules mobilized from Parylene C during annealing that diffuse through microvoids within platinum grain boundaries formed following platinum thin-film annealing [15, 16] and/or (2) a combination of the relaxation effects of the intrinsic residual stress of the deposited thin-film platinum [17] and possible formation of microcracks during thin-film platinum annealing [18]. Additional studies are underway to determine the cause of the altered electrochemical properties of thin film electrodes supported on thermoformed Parylene substrates.

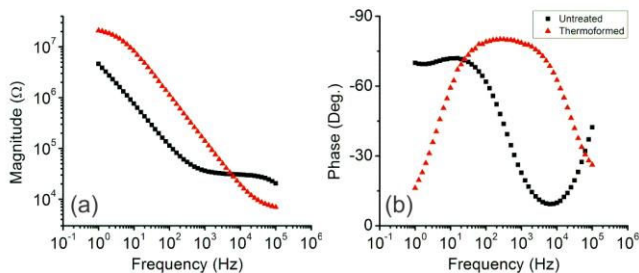


Figure 7. Representative plots impedance magnitude (a) and phase (b) of EIS measurements of untreated (red triangles) and thermoformed (black squares) electrode.

Despite the chemical or mechanical disruptions to the electrode surface caused by thermoforming, the electrodes were still able to detect resolvable neural signals *in vivo* as seen in Fig. 8.



Figure 8. Representative 500 msec trace from a 300-Hz high-pass filtered electrophysiological record from thermoformed PSE at 21 days post-implantation into the rat motor cortex.

IV. CONCLUSION

Evaluation of the chemical, mechanical, and electrochemical effects of the post-fabrication thermoforming process revealed little changes to the surface and bulk chemistry of the material, but an increase in material stiffness as well as alterations to the electrode surface. Despite these effects, the PSE still performed in its intended design as a sheath-based neural probe. Currently, additional studies are underway with more specific measurement methods to pinpoint the cause of the aberrant electrochemical effects of thermoforming. Although the PSE has been able to perform *in vivo* despite these factors, understanding the cause of the phenomenon may help in improving its chronic performance. Overall, our studies indicate that thermoforming is a simple process for achieving 3D Parylene C structures for neural interface applications with minimal effects on performance.

ACKNOWLEDGMENT

The authors would like to thank Dr. Saiyun Hou of the Huntington Medical Research Institutes (HMRI, Pasadena, CA 91105) for performing the chronic animal implantations and electrophysiological recordings, Mr. Yuzheng Zhang for aid in nanoindentation measurements, and the members of the USC Biomedical Microsystems Laboratory for their support.

REFERENCES

- [1] P. Abhishek and C. S. Justin, "Quantifying long-term microelectrode array functionality using chronic *in vivo* impedance testing," *Journal of Neural Engineering*, vol. 9, p. 026028, 2012.
- [2] G. C. McConnell, *et al.*, "Implanted neural electrodes cause chronic, local inflammation that is correlated with local neurodegeneration," *Journal of Neural Engineering*, vol. 6, Oct 2009.
- [3] D. H. Szarowski, *et al.*, "Brain responses to micro-machined silicon devices," *Brain Research*, vol. 983, pp. 23-35, Sep 5 2003.
- [4] J. N. Turner, *et al.*, "Cerebral astrocyte response to micro-machined silicon implants," *Experimental Neurology*, vol. 156, pp. 33-49, Mar 1999.
- [5] Y.-T. Kim, *et al.*, "Chronic response of adult rat brain tissue to implants anchored to the skull," *Biomaterials*, vol. 25, pp. 2229-2237, 2004.
- [6] J. T. W. Kuo, *et al.*, "Novel flexible Parylene neural probe with 3D sheath structure for enhancing tissue integration," *Lab on a Chip*, vol. 13, pp. 554-561, 2013.
- [7] P. R. Kennedy, *et al.*, "The cone electrode: ultrastructural studies following long-term recording in rat and monkey cortex," *Neuroscience letters*, vol. 142, pp. 89-94, 1992.
- [8] B. J. Kim, *et al.*, "Three dimensional transformation of Parylene thin film structures via thermoforming," in *Micro Electro Mechanical Systems (MEMS), 2013 IEEE 26th International Conference on*, 2013, pp. 339-342.
- [9] H.-S. Noh, *et al.*, "Parylene micromolding, a rapid and low-cost fabrication method for parylene microchannel," *Sensors and Actuators B*, vol. 102, pp. 78-85, 2004.
- [10] D. W. Grattan and M. Bilz, "The Thermal Aging of Parylene and the Effect of Antioxidant," *Studies in Conservation*, vol. 36, pp. 44-52, 1991.
- [11] R. Huang and Y. C. Tai, "Parylene to silicon adhesion enhancement," in *Solid-State Sensors, Actuators and Microsystems Conference, 2009. TRANSDUCERS 2009. International*, 2009, pp. 1027-1030.
- [12] S. F. Cogan, "Neural Stimulation and Recording Electrodes," *Annual Review of Biomedical Engineering*, vol. 10, pp. 275-309, 2008.
- [13] J.-M. Hsu, *et al.*, "Effect of Thermal and Deposition Processes on Surface Morphology, Crystallinity, and Adhesion of Parylene-C," *Sensors and Materials*, vol. 20, pp. 071-086, 2008.
- [14] B. J. Kim, *et al.*, "3D Parylene sheath neural probe for chronic recordings," *Journal of Neural Engineering*, vol. 10, p. 045002, 2013.
- [15] N. Beshchasna, *et al.*, "Influence of artificial body fluids and medical sterilization procedures on chemical stability of Parylene C," in *Electronic Components and Technology Conference (ECTC), 2010 Proceedings 60th*, 2010, pp. 1846-1852.
- [16] W. Gruber, *et al.*, "Strain Relaxation and Vacancy Creation in Thin Platinum Films," *Physical Review Letters*, vol. 107, p. 265501, 2011.
- [17] M. Grosser and U. Schmid, "The impact of annealing temperature and time on the electrical performance of Ti/Pt thin films," *Applied Surface Science*, vol. 256, pp. 4564-4569, 2010.
- [18] W. Sripumkhai, *et al.*, "Effect of Annealing Temperature on Platinum Thin Films Prepared by Electron Beam Evaporation," *Journal of the Microscopy Society of Thailand*, vol. 24, pp. 51-54, 2010.